

# Fully charmed resonance $X(6900)$ and its beauty counterpart

S. S. Agaev,<sup>1</sup> K. Azizi,<sup>2,3</sup> B. Barsbay,<sup>4</sup> and H. Sundu<sup>5</sup>

<sup>1</sup>*Institute for Physical Problems, Baku State University, Az-1148 Baku, Azerbaijan*

<sup>2</sup>*Department of Physics, University of Tehran, North Karegar Avenue, Tehran 14395-547, Iran*

<sup>3</sup>*Department of Physics, Doğuş University, Dudullu-Ümraniye, 34775 Istanbul, Türkiye*

<sup>4</sup>*Division of Optometry, School of Medical Services and Techniques, Doğuş University, 34775 Istanbul, Türkiye*

<sup>5</sup>*Department of Physics Engineering, Istanbul Medeniyet University, 34700 Istanbul, Türkiye*

(ΩDated: October 12, 2023)

The fully heavy scalar tetraquarks  $T_{4Q} = QQ\bar{Q}\bar{Q}$ , ( $Q = c, b$ ) are explored in the context of QCD sum rule method. We model  $T_{4Q}$  as diquark-antidiquark systems composed of pseudoscalar constituents, and calculate their masses  $m^{(\prime)}$  and couplings  $f^{(\prime)}$  within the two-point sum rule approach. Our results  $m = (6928 \pm 50)$  MeV and  $m' = (18858 \pm 50)$  MeV for masses of the tetraquarks  $T_{4c}$  and  $T_{4b}$  prove that they can decay to hidden-flavor heavy mesons. The full width  $\Gamma_{4c}$  of the  $T_{4c}$  is evaluated by taking into account the decay channels  $T_{4c} \rightarrow J/\psi J/\psi, J/\psi\psi', \eta_c\eta_c, \eta_c\eta_c(2S), \eta_c\chi_{c1}(1P)$ , and  $\chi_{c0}\chi_{c0}$ . The partial widths of these processes depend on strong couplings  $g_i$  at vertices  $T_{4c}J/\psi J/\psi, T_{4c}J/\psi\psi'$  etc., which are computed using the QCD three-point sum rule method. The decay  $T_{4b} \rightarrow \eta_b\eta_b$  is used to find the width  $\Gamma_{4b}$  of the  $T_{4b}$ . The predictions for  $m$  and  $\Gamma_{4c} = (128 \pm 22)$  MeV are compared with parameters of the fully charmed resonances reported by the LHCb, ATLAS, and CMS Collaborations. Based on this analysis, we interpret the tetraquark  $T_{4c}$  as a candidate to the resonance  $X(6900)$ . The mass  $m'$  and width  $\Gamma_{4b} = (94 \pm 28)$  MeV of the exotic meson  $T_{4b}$  can be used in future experimental investigations of these states.

## I. INTRODUCTION

It is known, that existence of exotic states composed of more than three valence partons or bearing unusual quantum numbers is not forbidden by the parton model and first principles of QCD. Phenomenological studies of such multi-quark hadrons started almost a half century ago from modeling the nonet of light scalar mesons as  $q^2\bar{q}^2$  four-quark states, and analysis of the doubly strange hexaquark structure [1, 2]. Due to collected experimental information and theoretical achievements multi-quark hadrons are objects of intensive studies in high energy physics.

Theoretical investigations of multi-quark hadrons aimed to elaborate methods to deal with such structures, calculate their parameters, and search for processes to detect them. One of important problems of these studies was a stability of multi-quark hadrons against strong and/or electromagnetic decays, because stable particles with long mean lifetimes can be easily observed in various processes. Structures composed of heavy  $QQ$  ( $Q = c$  or  $b$ ) diquarks and light antidiquarks are real candidates to such exotic mesons. Thus, it was already demonstrated that compounds  $QQ\bar{q}\bar{q}$  may be strong-interaction stable particles provided the ratio  $m_Q/m_q$  is large [3–5]. For example, a conclusion about stable nature of the isoscalar axial-vector tetraquark  $b\bar{b}\bar{u}d$  was made in Ref. [6] confirmed later by other researches [7–9]. Evidently stable tetraquarks transform to conventional mesons through weak processes, and live considerably longer than other multi-quark systems [10–19].

The heavy exotic mesons  $QQ\bar{Q}^{(\prime)}\bar{Q}^{(\prime)}$  establish another class of particles, which deserves detailed theoretical and experimental investigations. Recently, the LHCb, ATLAS and CMS Collaborations reported new structures

discovered in di- $J/\psi$  and  $J/\psi\psi'$  mass distributions [20–22]. The LHCb observed a threshold enhancement in nonresonant di- $J/\psi$  production from 6.2 to 6.8 GeV with center at 6.49 GeV. A narrow peak  $X(6900)$  at 6.9 GeV, and a resonance around 7.2 GeV were seen as well. The ATLAS and CMS experiments detailed information on structures in the region 6.2 – 6.8 GeV and at 7.2 GeV. Thus, ATLAS detected the resonances  $X(6200)$ ,  $X(6600)$ , and  $X(6900)$  in the di- $J/\psi$  and  $X(7300)$  in the  $J/\psi\psi'$  channels, respectively. The resonances  $X(6600)$ ,  $X(6900)$  and  $X(7300)$  were fixed by the CMS Collaboration as well.

Analyses performed in the context of various methods and models led to interesting, sometimes to contradictory interpretations of the observed resonances [23–34]. In fact,  $X(6900)$  was interpreted as a tetraquark built of pseudoscalar diquark and antidiquark components [24]. The  $X(6200)$  was assigned to be the ground-level tetraquark state with  $J^{PC} = 0^{++}$  or  $1^{+-}$ , whereas  $X(6600)$  was considered as its first radial excitation [25]. In Ref. [26] the authors proposed to consider the resonances, starting from  $X(6200)$ , as the  $1S$ ,  $1P/2S$ ,  $1D/2P$ , and  $2D/3P/4S$  tetraquark states. Similar interpretations in the context of the relativistic quark model were suggested as well [27]. The resonance  $X(6900)$  was modeled as hadronic molecules  $\chi_{c0}\chi_{c0}$  or  $J/\psi\psi(3770)$ ,  $\chi_{c0}\chi_{c2}$  in Refs. [24, 28], respectively.

Alternatively, in the framework of the coupled-channel approach a near-threshold state in the di- $J/\psi$  system with  $J^{PC} = 0^{++}$  or  $J^{PC} = 2^{++}$  was interpreted as  $X(6200)$  [29]. Coupled-channel effects may also generate a pole structure identified in Ref. [30] with the resonance  $X(6900)$ . The  $X(6900)$  may be dynamically generated by the Pomeron exchanges and coupled-channel effects between the  $J/\psi J/\psi$  and  $J/\psi\psi'$  scattering [31].

In our article [35], we carried out rather detailed analysis of the fully charmed  $X_{4c}$  and beauty  $X_{4b}$  scalar four-quark mesons by calculating their masses and current couplings. We modeled  $X_{4c}$  and  $X_{4b}$  as diquark-antidiquarks built of axial-vector constituents  $Q^T C \gamma_\mu Q$  and  $\bar{Q} \gamma^\mu C \bar{Q}^T$  (briefly, a tetraquark with a structure  $C \gamma_\mu \otimes \gamma^\mu C$ ), where  $C$  is the charge conjugation matrix. Our prediction for the mass  $m = (6570 \pm 55)$  MeV of the tetraquark  $X_{4c}$  proved that it can decay to  $J/\psi J/\psi$ ,  $\eta_c \eta_c$ , and  $\eta_c \chi_{c1}(1P)$  mesons. The full width of  $X_{4c}$  was computed using these decay modes and found equal to  $\Gamma_{4c} = (110 \pm 21)$  MeV. Comparison with available data allowed us to consider  $X_{4c}$  as a candidate to the resonance  $X(6600)$ . We also argued that  $X(7300)$  may be considered as  $2S$  excitation of the resonance  $X(6600)$ . In Ref. [35], we calculated the mass of the fully beauty scalar state  $X_{4b}$  as well. It turned out that, its mass  $m' = (18540 \pm 50)$  MeV is below the  $\eta_b \eta_b$  threshold, and hence  $X_{4b}$  can not decay to pairs of hidden-beauty mesons. Its decays run via a  $\bar{b}b$  transformation to a gluon(s) and light quark-antiquark pairs followed by creation of ordinary  $B$  mesons [36, 37]. The electroweak leptonic and nonleptonic decays of  $X_{4b}$  are also among its possible transitions to conventional particles.

In the present work, we continue our explorations of the LHCb-ATLAS-CMS resonances in the context of the diquark-antidiquark model. We compute parameters of the scalar  $J^{PC} = 0^{++}$  state  $T_{4c}$  built of pseudoscalar diquark components, i. e., a tetraquark with  $C \otimes C$  type internal organization. We calculate the mass and full width of  $T_{4c}$ , and confront our results with the experimental data for the fully charmed  $X$  resonances. We investigate also its beauty counterpart  $T_{4b}$  to determine the mass and width of this state.

The current paper is organized in the following manner: In Section II, we calculate the mass and current coupling of the tetraquarks  $T_{4c}$  and  $T_{4b}$ . In Sec. III, we consider decays of  $T_{4c}$  to mesons  $J/\psi J/\psi$  and  $J/\psi \psi'$ . The processes  $T_{4c} \rightarrow \eta_c \eta_c$ ,  $\eta_c \eta_c(2S)$  are analyzed in Sec. IV. The decays  $T_{4c} \rightarrow \eta_c \chi_{c1}(1P)$  and  $T_{4c} \rightarrow \chi_{c0} \chi_{c0}$  are investigated in Sec. V. Here, we also determine the full width of  $T_{4c}$ . The width of the process  $T_{4b} \rightarrow \eta_b \eta_b$  is computed in Sec. VI. Last section is reserved for discussion of results and contains our concluding notes.

## II. MASS AND CURRENT COUPLING OF THE TETRAQUARKS $T_{4c}$ AND $T_{4b}$

Here, we compute the masses  $m^{(\prime)}$  and current couplings  $f^{(\prime)}$  of the exotic fully heavy-flavor mesons  $T_{4c}$  and  $T_{4b}$  in the context of the QCD two-point sum rule method [38, 39]. To this end, we consider the correlation function

$$\Pi(p) = i \int d^4x e^{ipx} \langle 0 | \mathcal{T} \{ J(x) J^\dagger(0) \} | 0 \rangle, \quad (1)$$

where,  $\mathcal{T}$  is the time-ordered product of two currents, and  $J(x)$  is the interpolating currents for these states.

We treat  $T_{4c}$  and  $T_{4b}$  as tetraquarks built of pseudoscalar diquark  $Q^T C Q$  and antidiquark  $\bar{Q} C \bar{Q}^T$ . Then relevant interpolating current is defined by the expression

$$J(x) = Q_a^T(x) C Q_b(x) \bar{Q}_a(x) C \bar{Q}_b^T(x), \quad (2)$$

where  $a$ , and  $b$  are color indices, and  $Q(x)$  is either  $c$  or  $b$  quark field. The current  $J(x)$  describes the diquark-antidiquark state with quantum numbers  $J^{PC} = 0^{++}$ .

Below, we present formulas for the four-quark state  $T_{4c}$ , which can be readily extended to the case of  $T_{4b}$ . The phenomenological side of the sum rule  $\Pi^{\text{Phys}}(p)$  can be found from Eq. (1) by inserting a complete set of intermediate states with quark content and spin-parities of the tetraquark  $T_{4c}$ , and carrying out integration over  $x$ . As a result, we get

$$\Pi^{\text{Phys}}(p) = \frac{\langle 0 | J | T_{4c}(p) \rangle \langle T_{4c}(p) | J^\dagger | 0 \rangle}{m^2 - p^2} + \dots, \quad (3)$$

where  $p$  is four-momentum of  $T_{4c}$ . The dots in Eq. (3) denote contributions of higher resonances and continuum states.

The correlation function  $\Pi^{\text{Phys}}(p)$  can be rewritten in terms of the tetraquark's parameters through

$$\langle 0 | J | T_{4c}(p) \rangle = f m, \quad (4)$$

which gives

$$\Pi^{\text{Phys}}(p) = \frac{f^2 m^2}{m^2 - p^2} + \dots. \quad (5)$$

The correlator  $\Pi^{\text{Phys}}(p)$  has a Lorentz structure which is proportional to I. Then, an invariant amplitude  $\Pi^{\text{Phys}}(p^2)$  required to derive the sum rules is equal to right-hand side of Eq. (5).

The counterpart of  $\Pi^{\text{Phys}}(p^2)$ , i.e., the invariant amplitude  $\Pi^{\text{OPE}}(p^2)$  evaluated by employing the heavy quark propagators establishes the QCD side of the sum rule. The function  $\Pi^{\text{OPE}}(p^2)$  is extracted from the correlator  $\Pi^{\text{OPE}}(p)$  that is calculated in the operator product expansion (OPE) and contains only a component proportional to I.

In terms of  $c$ -quark propagators  $\Pi^{\text{OPE}}(p)$  is given by the formula

$$\begin{aligned} \Pi^{\text{OPE}}(p) = & i \int d^4x e^{ipx} \left\{ \text{Tr} \left[ \tilde{S}_c^{b'b}(-x) S_c^{a'a}(-x) \right] \right. \\ & \times \left[ \text{Tr} \left[ \tilde{S}_c^{aa'}(x) S_c^{bb'}(x) \right] + \text{Tr} \left[ \tilde{S}_c^{ba'}(x) \right. \right. \\ & \left. \left. \times S_c^{ab'}(x) \right] \right] + \text{Tr} \left[ \tilde{S}_c^{a'b}(-x) S_c^{b'a}(-x) \right] \\ & \left. \times \left[ \text{Tr} \left[ \tilde{S}_c^{ba'}(x) S_c^{ab'}(x) \right] + \text{Tr} \left[ \tilde{S}_c^{aa'}(x) S_c^{bb'}(x) \right] \right] \right\}. \end{aligned} \quad (6)$$

Here,

$$\tilde{S}_c(x) = C S_c^T(x) C, \quad (7)$$

and  $S_c(x)$  is the  $c$ -quark propagator explicit expression of which can be found in Appendix (see, also Refs. [35, 40]).

At the next stage of analysis, we equate the amplitudes  $\Pi^{\text{Phys}}(p^2)$  and  $\Pi^{\text{OPE}}(p^2)$ , apply the Borel transformation to suppress effects of higher resonances and continuum states, and make use of the assumption on quark-hadron duality to subtract these terms from the physical side of the sum rule equality. After some trivial manipulations, we derive the following sum rules for the mass  $m$  and current coupling  $f$  of the tetraquark  $T_{4c}$

$$m^2 = \frac{\Pi'(M^2, s_0)}{\Pi(M^2, s_0)} \quad (8)$$

and

$$f^2 = \frac{e^{m^2/M^2}}{m^2} \Pi(M^2, s_0), \quad (9)$$

where  $\Pi'(M^2, s_0) = d\Pi(M^2, s_0)/d(-1/M^2)$ . In Eqs. (8) and (9) the function  $\Pi(M^2, s_0)$  is the amplitude  $\Pi^{\text{OPE}}(p^2)$  obtained after the Borel transformation and continuum subtraction procedures. It depends on the Borel  $M^2$  and continuum subtraction  $s_0$  parameters, which appear in the sum rule equality after corresponding operations.

The function  $\Pi(M^2, s_0)$  has the form

$$\Pi(M^2, s_0) = \int_{16m^2}^{s_0} ds \rho^{\text{OPE}}(s) e^{-s/M^2}, \quad (10)$$

where  $\rho^{\text{OPE}}(s)$  is a two-point spectral density determined as an imaginary part of the invariant amplitude  $\Pi^{\text{OPE}}(p^2)$ . In general, the operator production expansion for the correlation function  $\Pi^{\text{OPE}}(p)$ , apart from the perturbative term, contains contributions of gluon condensates  $\sim \langle \alpha_s G^2/\pi \rangle$ ,  $\langle g_s^3 G^3 \rangle$  etc. Because effects of higher dimensional terms are numerically small, we restrict ourselves by considering only dimension-4 contribution, which is proportional to  $\langle \alpha_s G^2/\pi \rangle$ . As a result, the function  $\rho^{\text{OPE}}(s)$  consists of a perturbative term  $\rho^{\text{pert.}}(s)$  and a dimension-4 nonperturbative contribution  $\sim \langle \alpha_s G^2/\pi \rangle$

$$\rho^{\text{OPE}}(s) = \rho^{\text{pert.}}(s) + \langle \frac{\alpha_s G^2}{\pi} \rangle \rho^{\text{Dim4}}(s). \quad (11)$$

The explicit expression of  $\rho^{\text{pert.}}(s)$  is written down in Appendix. The function  $\rho^{\text{Dim4}}(s)$  is rather lengthy and, therefore, has not been provided there.

In the case under discussion,  $\Pi^{\text{OPE}}(p)$  depends only the  $c$ -quark propagators, which does not contain the light quark and mixed quark-gluon condensates. As a result, we need for numerical analysis of the sum rules the masses of  $c$  and  $b$  quarks, as well as the gluon vacuum condensate  $\langle \alpha_s G^2/\pi \rangle$ : Values of these parameters are presented below

$$\begin{aligned} m_c &= (1.27 \pm 0.02) \text{ GeV}, \\ m_b &= 4.18_{-0.02}^{+0.03} \text{ GeV}, \\ \langle \frac{\alpha_s G^2}{\pi} \rangle &= (0.012 \pm 0.004) \text{ GeV}^4. \end{aligned} \quad (12)$$

One should also fix the working regions for parameters  $M^2$  and  $s_0$ . The  $M^2$  and  $s_0$  have to satisfy constraints imposed on  $\Pi(M^2, s_0)$  by a pole contribution (PC) and convergence of the operator product expansion. To evaluate PC, we employ the expression

$$\text{PC} = \frac{\Pi(M^2, s_0)}{\Pi(M^2, \infty)}, \quad (13)$$

and require fulfillment of the constraint  $\text{PC} \geq 0.5$ .

Because the sum rules for  $m$  and  $f$  depend only on a nonperturbative term  $\sim \langle \alpha_s G^2/\pi \rangle$ , the pole contribution becomes an important criterium in the choice of  $M^2$  and  $s_0$ . We demand also a stability of extracted observables under variations of the Borel and continuum subtraction parameters. In fact,  $M^2$  and  $s_0$  are the auxiliary quantities in computations, therefore, the physical observables should not depend on  $M^2$  and  $s_0$ . In real analysis, however,  $m$  and  $f$  bear such residual dependence. Hence, the maximal stability of  $m$  and  $f$  under variations of  $M^2$  and  $s_0$  is among important constraints in the choice of relevant working intervals. The prevalence of a perturbative contribution over nonperturbative one is a required condition as well.

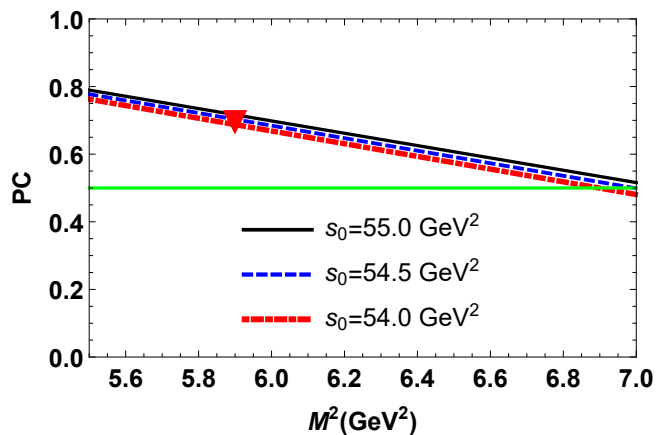


FIG. 1: The pole contribution PC as a function of the Borel parameter  $M^2$  at different  $s_0$ . The limit  $\text{PC} = 0.5$  is plotted by the horizontal line. The red triangle shows the point, where the mass  $m$  of the tetraquark  $T_{4c}$  has been extracted from the sum rule.

By employing PC one can fix the higher limit of the Borel parameter  $M^2$ . The lower border for  $M^2$  is found from a stability of the sum rules' results under variation of  $M^2$ , and from superiority of the perturbative term in extracted quantities. Two values of  $M^2$  determined by this manner limit the region where  $M^2$  can be changed. Numerical computations demonstrate that the regions

$$M^2 \in [5.5, 7] \text{ GeV}^2, \quad s_0 \in [54, 55] \text{ GeV}^2, \quad (14)$$

meet all necessary constraints imposed on the correlation function by the sum rule analyses. Thus, at  $M^2 = 5.5 \text{ GeV}^2$  and  $M^2 = 7 \text{ GeV}^2$  the pole contribution equals to 0.78 and 0.51, respectively. In order to show

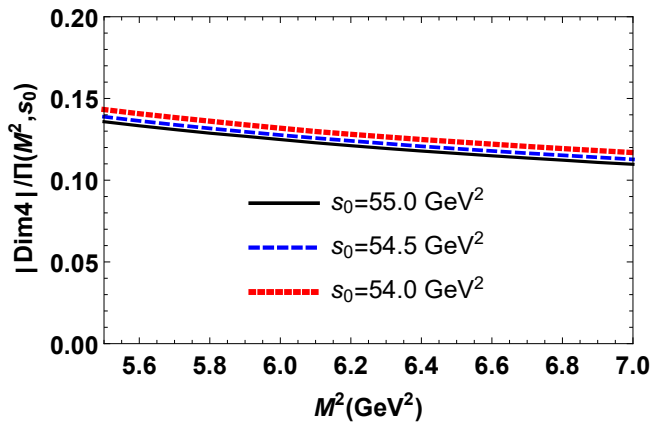


FIG. 2: The ratio of the nonperturbative  $|\Pi^{\text{Dim4}}(M^2, s_0)|$  contribution and the whole  $\Pi(M^2, s_0)$  correlation function as a function of the Borel parameter at fixed  $s_0$ .

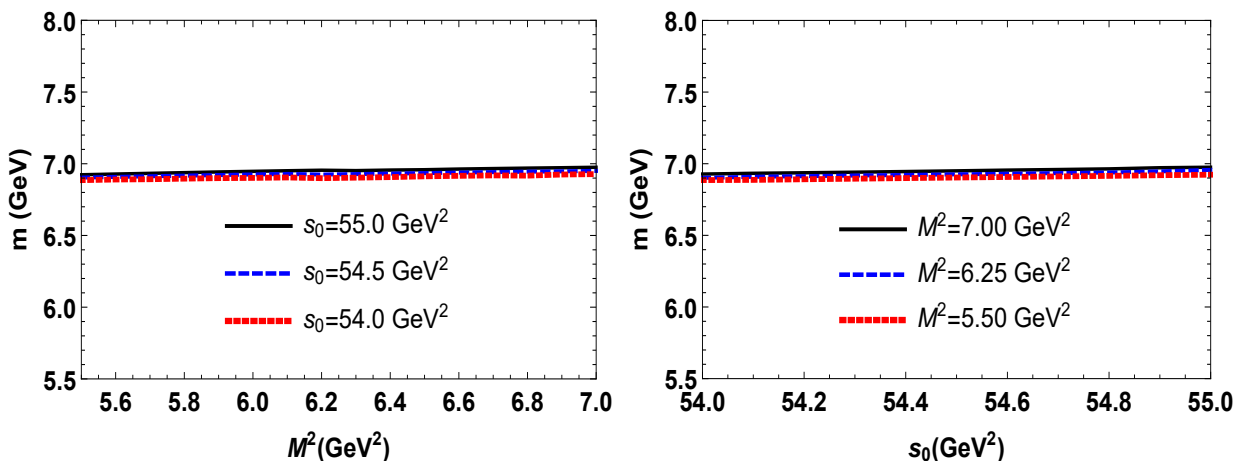


FIG. 3: Mass of the tetraquark  $T_{4c}$  as a function of the Borel  $M^2$  (left), and the continuum threshold  $s_0$  parameters (right).

The region for  $s_0$  has to comply with constraints coming from the dominance of PC and prevalence of perturbative term in OPE. Besides,  $s_0$  separates contributions of the ground-level  $T_{4c}$  and first excited tetraquark  $T_{4c}^*$  with the mass  $m^*$ , therefore the inequalities  $m < \sqrt{s_0} < m^*$  should be satisfied. These restrictions provide an opportunity to verify self-consistency of performed studies and correctness of the chosen region for  $s_0$ . Additionally, using  $\sqrt{s_0} < m^*$  it is possible to estimate lower limit for the mass of the excited state  $T_{4c}^*$ . In the lack of experimental and theoretical information on parameters of excited tetraquarks, this is one of useful ways to gain some knowledge about the mass of the first excited diquark-antidiquark state  $T_{4c}^*$ .

The mass  $m$  and current coupling  $f$  of the tetraquark  $T_{4c}$  are calculated as values of these parameters averaged

dynamics of the pole contribution, in Fig. 1 we depict PC as a function of  $M^2$  at different  $s_0$ : It exceeds 0.5 for all values of the parameters  $M^2$  and  $s_0$  from Eq. (14).

The nonperturbative term  $\Pi^{\text{Dim4}}(M^2, s_0)$  is negative, and at the minimum  $M^2 = 5.5 \text{ GeV}^2$  forms 14% of the correlation function gradually decreasing with  $M^2$  (see, Fig. 2). The next term  $\sim \langle g_s^3 G^3 \rangle$  in OPE would be considerably smaller than the dimension-4 contribution and is neglected almost in all sum rule analysis of fully heavy tetraquarks.

over the regions (14). Our results for  $m$  and  $f$  are:

$$\begin{aligned} m &= (6928 \pm 50) \text{ MeV}, \\ f &= (2.06 \pm 0.14) \times 10^{-2} \text{ GeV}^4. \end{aligned} \quad (15)$$

It is seen, that ambiguities of calculations are very small and are equal to  $\pm 1\%$  for the mass and  $\pm 7\%$  in the case of the current coupling. The results Eq. (15) correspond to sum rules' predictions at the point  $M^2 = 5.9 \text{ GeV}^2$  and  $s_0 = 54.5 \text{ GeV}^2$ , where the pole contribution is  $\text{PC} \approx 0.7$  (see, Fig. 1). This fact ensures dominance of PC in extracted quantities, and ground-state nature of the exotic meson  $T_{4c}$ . The mass  $m$  of the tetraquark  $T_{4c}$  is plotted in Fig. 3.

The dependence of the mass  $m$  on the continuum threshold parameter  $s_0$  can be seen in the right panel of Fig. 3. It is not difficult to be convinced in self-

consistency of the present calculations. Indeed, with the result for  $m$  at hand, one sees that  $m < \sqrt{s_0}$ . It is also easy to find  $m^* > m + 450$  MeV, which for a particle containing four  $c$  quarks seem is a reasonable estimate.

Our result for  $m$  is in excellent agreement with the mass of the resonance  $X(6900)$  measured by the CMS collaboration. It is also compatible with LHCb and ATLAS data though slightly exceeds them. But for detailed comparison with available data, and more reliable conclusions on nature of  $T_{4c}$ , we have to estimate its full width.

In the case of the tetraquark  $T_{4b}$  for  $M^2$  and  $s_0$  computations give the following regions

$$\begin{aligned} M^2 &\in [17.5, 18.5] \text{ GeV}^2, \\ s_0 &\in [380, 385] \text{ GeV}^2. \end{aligned} \quad (16)$$

Here, the PC varies within the interval

$$0.64 \geq \text{PC} \geq 0.58. \quad (17)$$

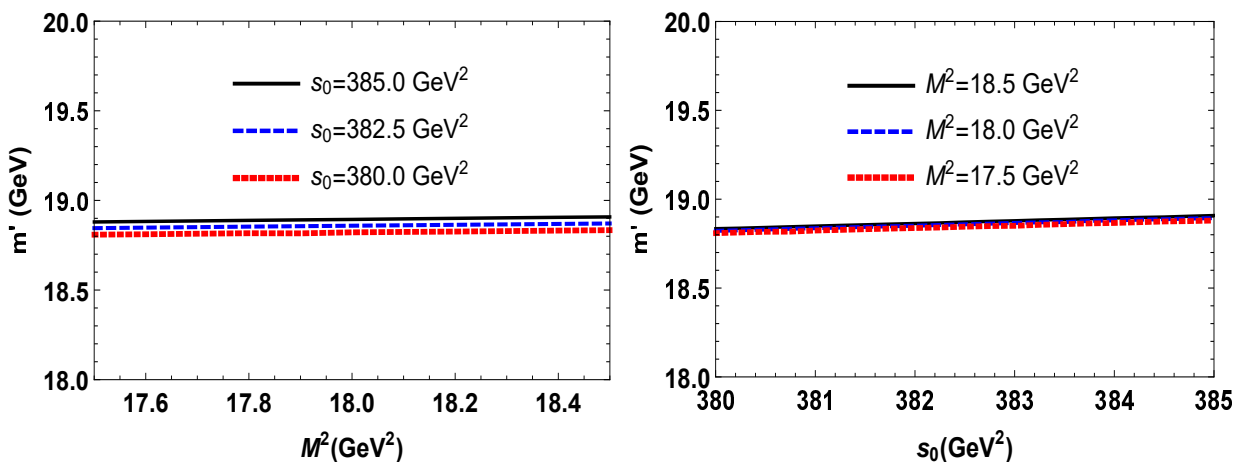


FIG. 4: Mass  $m'$  of the tetraquark  $T_{4b}$  as a function of the parameters  $M^2$  (left), and  $s_0$  (right).

### III. DECAYS $T_{4c} \rightarrow J/\psi J/\psi$ AND $T_{4c} \rightarrow J/\psi \psi'$

The prediction for the mass of the diquark-antidiquark system with structure  $C \otimes C$  permits us to determine kinematically allowed decay modes of  $T_{4c}$ . The mass  $m = 6928$  MeV of this tetraquark exceeds the two-meson  $J/\psi J/\psi$  and  $J/\psi \psi'$  thresholds. The  $m$  satisfies also the kinematical restrictions for productions of  $\eta_c \eta_c$  and  $\eta_c \eta_c(2S)$  pairs.  $T_{4c}$  can decay to conventional  $\eta_c \chi_{c1}(1P)$  and  $\chi_{c0} \chi_{c0}$  mesons as well. The decay  $T_{4c} \rightarrow \eta_c \chi_{c1}(1P)$  is  $P$ -wave, whereas remaining five channels are  $S$ -wave processes.

We start our studies from investigation of the decays  $J/\psi J/\psi$  and  $J/\psi \psi'$ . The three-point sum rules

The dimension-4 term constitutes  $-2.2\%$  of the result at  $M^2 = 17.5 \text{ GeV}^2$ . The mass and current coupling of the fully beauty tetraquark  $T_{4b}$  are equal to

$$\begin{aligned} m' &= (18858 \pm 50) \text{ MeV}, \\ f' &= (9.54 \pm 0.71) \times 10^{-2} \text{ GeV}^4. \end{aligned} \quad (18)$$

Behavior of  $m'$  as a function of  $M^2$  and  $s_0$  is shown in Fig. 4.

The diquark-antidiquark state  $T_{4b}$  with  $C \otimes C$  structure and mass  $m' = 18858$  MeV is above  $\eta_b \eta_b$  but below  $\Upsilon(1S)\Upsilon(1S)$  thresholds. Consequently, it decays to a  $\eta_b \eta_b$  pair and may be searched for in invariant mass distributions of these mesons.

for the strong form factors  $g_1(q^2)$  and  $g_1^*(q^2)$  which describe interaction of particles at vertices  $T_{4c} J/\psi J/\psi$  and  $T_{4c} J/\psi \psi'$  respectively, can be extracted from analysis of the correlation function

$$\begin{aligned} \Pi_{\mu\nu}(p, p') &= i^2 \int d^4x d^4y e^{ip'y} e^{-ipx} \langle 0 | \mathcal{T} \{ J_\mu^\psi(y) \\ &\times J_\nu^\psi(0) J^\dagger(x) \} | 0 \rangle, \end{aligned} \quad (19)$$

where the current  $J(x)$  is defined by Eq. (2), and  $J_\mu^\psi(x)$  is the interpolating currents for the mesons  $J/\psi$  and  $\psi'$

$$J_\mu^\psi(x) = \bar{c}_i(x) \gamma_\mu c_i(x), \quad (20)$$

where  $i = 1, 2, 3$  are the color indices.

We apply usual recipes of the sum rule method and write down the correlation function  $\Pi_{\mu\nu}(p, p')$  in terms of physical parameters of particles. Because the tetraquark  $T_{4c}$  can decay both to  $J/\psi J/\psi$  and  $J/\psi \psi'$  pairs, we isolate in  $\Pi_{\mu\nu}(p, p')$  contributions of the particles  $J/\psi$  and  $\psi'$  from higher resonances and continuum states' effects. Then, for the phenomenological component of the sum rule  $\Pi_{\mu\nu}^{\text{Phys}}(p, p')$ , we get

$$\begin{aligned} \Pi_{\mu\nu}^{\text{Phys}}(p, p') &= \frac{\langle 0 | J_\mu^\psi | J/\psi(p') \rangle \langle 0 | J_\nu^\psi | J/\psi(q) \rangle}{p'^2 - m_1^2} \frac{\langle 0 | J_\nu^\psi | J/\psi(q) \rangle}{q^2 - m_1^2} \\ &\times \langle J/\psi(p') J/\psi(q) | T_{4c}(p) \rangle \frac{\langle T_{4c}(p) | J^\dagger | 0 \rangle}{p^2 - m^2} \\ &+ \frac{\langle 0 | J_\mu^\psi | \psi(p') \rangle \langle 0 | J_\nu^\psi | J/\psi(q) \rangle}{p'^2 - m_1^{*2}} \frac{\langle 0 | J_\nu^\psi | J/\psi(q) \rangle}{q^2 - m_1^2} \\ &\times \langle \psi(p') J/\psi(q) | T_{4c}(p) \rangle \frac{\langle T_{4c}(p) | J^\dagger | 0 \rangle}{p^2 - m^2} + \dots, \quad (21) \end{aligned}$$

with  $m_1$  and  $m_1^*$  being the masses of  $J/\psi$  and  $\psi'$  mesons.

The function  $\Pi_{\mu\nu}^{\text{Phys}}(p, p')$  can be rewritten using the matrix elements of the tetraquark  $T_{4c}$ , and mesons  $J/\psi$  and  $\psi'$ . The matrix element of  $T_{4c}$  is given by Eq. (4), whereas for  $\langle 0 | J_\mu^\psi | J/\psi(p) \rangle$  and  $\langle 0 | J_\mu^\psi | \psi'(p) \rangle$ , we utilize

$$\begin{aligned} \langle 0 | J_\mu^\psi | J/\psi(p) \rangle &= f_1 m_1 \varepsilon_\mu(p), \\ \langle 0 | J_\mu^\psi | \psi'(p) \rangle &= f_1^* m_1^* \tilde{\varepsilon}_\mu(p), \quad (22) \end{aligned}$$

where  $f_1$ ,  $f_1^*$ , and  $\varepsilon_\mu$ ,  $\tilde{\varepsilon}$  are the decay constants and polarization vectors of  $J/\psi$  and  $\psi'$ , respectively.

For the vertices, we employ the following expressions

$$\begin{aligned} \langle J/\psi(p') J/\psi(q) | T_{4c}(p) \rangle &= g_1(q^2) [q \cdot p' \varepsilon^*(p') \cdot \varepsilon^*(q) \\ &- q \cdot \varepsilon^*(p') p' \cdot \varepsilon^*(q)], \quad (23) \end{aligned}$$

and

$$\begin{aligned} \langle \psi(p') J/\psi(q) | T_{4c}(p) \rangle &= g_1^*(q^2) [q \cdot p' \tilde{\varepsilon}^*(p') \cdot \varepsilon^*(q) \\ &- q \cdot \tilde{\varepsilon}^*(p') p' \cdot \varepsilon^*(q)]. \quad (24) \end{aligned}$$

Having utilized these matrix elements and carried out simple calculations, for  $\Pi_{\mu\nu}^{\text{Phys}}(p, p')$  we find

$$\begin{aligned} \Pi_{\mu\nu}^{\text{Phys}}(p, p') &= g_1(q^2) \frac{f m f_1^2 m_1^2}{(p^2 - m^2)(p'^2 - m_1^2)(q^2 - m_1^2)} \\ &\times \left[ \frac{1}{2} (m^2 - m_1^2 - q^2) g_{\mu\nu} - q_\mu p'_\nu \right] + \\ &+ g_1^*(q^2) \frac{f m f_1 m_1 f_1^* m_1^*}{(p^2 - m^2)(p'^2 - m_1^{*2})(q^2 - m_1^2)} \\ &\times \left[ \frac{1}{2} (m^2 - m_1^{*2} - q^2) g_{\mu\nu} - q_\mu p'_\nu \right] + \dots, \quad (25) \end{aligned}$$

where contributions of higher resonances and continuum states are denoted by the dots. The function  $\Pi_{\mu\nu}^{\text{Phys}}(p, p')$  contains the Lorentz structures, which are proportional to  $g_{\mu\nu}$  and  $q_\mu p'_\nu$ . Both of them can be employed to determine the sum rules for  $g_1(q^2)$  and  $g_1^*(q^2)$ . We work with

Parameters	Values (in MeV)
$m_1[m_{J/\psi}]$	$3096.900 \pm 0.006$
$f_1[f_{J/\psi}]$	$409 \pm 15$
$m_1^*[m_{\psi'}]$	$3686.10 \pm 0.06$
$f_1^*[f_{\psi'}]$	$279 \pm 8$
$m_2[m_{\eta_c}]$	$2983.9 \pm 0.4$
$f_2[f_{\eta_c}]$	$398.1 \pm 1.0$
$m_2^*[m_{\eta_c(2S)}]$	$3637.5 \pm 1.1$
$f_2^*[f_{\eta_c(2S)}]$	$331$
$m_3[m_{\chi_{c1}}]$	$3510.67 \pm 0.05$
$f_3[f_{\chi_{c1}}]$	$344 \pm 27$
$m_4[m_{\chi_{c0}}]$	$3414.71 \pm 0.30$
$f_4[f_{\chi_{c0}}]$	$343$
$m_5[m_{\eta_b}]$	$9398.7 \pm 2.0$
$f_5[f_{\eta_b}]$	$724 \pm 12$

TABLE I: Masses and decay constants of the various charmonia and  $\eta_b$  meson, which have been used in numerical computations.

the structures  $\sim g_{\mu\nu}$  and denote the relevant invariant amplitudes by  $\Pi_1^{\text{Phys}}(p^2, p'^2, q^2)$  and  $\Pi_2^{\text{Phys}}(p^2, p'^2, q^2)$ , respectively. Then, a total amplitude  $\Pi^{\text{Phys}}(p^2, p'^2, q^2)$  is equal to a sum of the functions  $\Pi_{1,2}^{\text{Phys}}(p^2, p'^2, q^2)$ . The Borel transformations of  $\Pi^{\text{Phys}}(p^2, p'^2, q^2)$  over  $-p^2$  and  $-p'^2$  give

$$\begin{aligned} B\Pi^{\text{Phys}}(p^2, p'^2, q^2) &= g_1(q^2) f m f_1^2 m_1^2 \\ &\times \frac{m^2 - m_1^2 - q^2}{2(q^2 - m_1^2)} e^{-m^2/M_1^2} e^{-m_1^2/M_2^2} \\ &+ g_1^*(q^2) f m f_1 m_1 f_1^* m_1^* \frac{m^2 - m_1^{*2} - q^2}{2(q^2 - m_1^2)} \\ &\times e^{-m^2/M_1^2} e^{-m_1^{*2}/M_2^2} + \dots. \quad (26) \end{aligned}$$

The correlation function  $\Pi_{\mu\nu}(p, p')$  expressed using the  $c$ -quark propagators

$$\begin{aligned} \Pi_{\mu\nu}^{\text{OPE}}(p, p') &= 2i^2 \int d^4x d^4y e^{ip'y} e^{-ipx} \\ &\times \left\{ \text{Tr} \left[ \gamma_\mu S_c^{ib}(y-x) \tilde{S}_c^{ja}(-x) \gamma_\nu \tilde{S}_c^{bj}(x) S_c^{ai}(x-y) \right] \right. \\ &\left. + \text{Tr} \left[ \gamma_\mu S_c^{ia}(y-x) \tilde{S}_c^{jb}(-x) \gamma_\nu \tilde{S}_c^{bj}(x) S_c^{ai}(x-y) \right] \right\}, \quad (27) \end{aligned}$$

is the QCD side of the sum rule.

The invariant amplitude  $\Pi^{\text{OPE}}(p^2, p'^2, q^2)$  obtained from the component  $\sim g_{\mu\nu}$  of Eq. (27) can be used in following studies. By equating the double Borel transforms of the amplitudes  $\Pi^{\text{OPE}}(p^2, p'^2, q^2)$  and  $\Pi^{\text{Phys}}(p^2, p'^2, q^2)$ , and carrying out the continuum subtraction, one can find the sum rules for the form factors  $g_1(q^2)$  and  $g_1^*(q^2)$ .

After the Borel transformation and continuum subtraction,  $\Pi^{\text{OPE}}(p^2, p'^2, q^2)$  can be written down in terms of

the spectral density  $\rho(s, s', q^2)$  determined as a relevant imaginary part of  $\Pi_{\mu\nu}^{\text{OPE}}(p, p')$

$$\Pi(\mathbf{M}^2, \mathbf{s}_0, q^2) = \int_{16m_c^2}^{s_0} ds \int_{4m_c^2}^{s'_0} ds' \rho(s, s', q^2) \times e^{-s/M_1^2} e^{-s'/M_2^2}. \quad (28)$$

Here,  $\mathbf{M}^2 = (M_1^2, M_2^2)$  and  $\mathbf{s}_0 = (s_0, s'_0)$  are the Borel and continuum threshold parameters, respectively. The pair of parameters  $(M_1^2, s_0)$  corresponds to the tetraquark channel, the pair  $(M_2^2, s'_0)$  – to the  $J/\psi$  ( $\psi'$ ) channel.

To extract the sum rules for  $g_1(q^2)$  and  $g_1^*(q^2)$ , at the first stage of analysis, we fix the continuum subtraction parameter as  $4m_c^2 < s'_0 < m_1^{*2}$ , where  $m_1^*$  is the mass of the excited  $\psi' = \psi(2^3S_1)$  meson. By this way, we include the second term in Eq. (26) into higher resonances and continuum states. This scheme is the standard "ground-state + continuum" approach, when the physical side of the sum rule contains a contribution coming only from ground-state particles. Then, it is not difficult to derive the sum rule for the form factor  $g_1(q^2)$

$$g_1(q^2) = \frac{2}{f m f_1^2 m_1^2} \frac{q^2 - m_1^2}{m^2 - m_1^2 - q^2} \times e^{m^2/M_1^2} e^{m_1^2/M_2^2} \Pi(\mathbf{M}^2, \mathbf{s}_0, q^2). \quad (29)$$

At the next phase of calculations, we choose  $m_1^{*2} < s_0^{*'} < m^{**2}$ , with  $m^{**} = (4039 \pm 1)$  MeV being the mass of the next excited state  $\psi(3^3S_1)$  [41, 42]. By this way, we include into consideration the second term in Eq. (26): This is "ground-state + excited state + continuum" scheme. Afterwards, by employing results obtained for  $g_1(q^2)$  one can determine  $g_1^*(q^2)$ .

All information necessary for numerical computations of the form factors  $g_1(q^2)$  and  $g_1^*(q^2)$  are collected in Table I. In this Table, we present parameters of the  $\eta_c$ ,  $\eta_c(2S)$ ,  $\chi_{c1}(1P)$ , and  $\eta_b$  mesons that will be used later to explore decays of  $T_{4c}$  and  $T_{4b}$ . The masses of the particles are borrowed from Ref. [41]. For decay constant of the meson  $J/\psi$ , we employ the experimental value reported in Ref. [43]. As  $f_{\eta_c}$  and  $f_{\eta_b}$ , we use results of QCD lattice simulations [44, 45], whereas for  $f_{\chi_{c1}}$  and  $f_{\chi_{c0}}$  – the sum rule predictions from Refs. [46, 47].

To perform numerical computations, we also have to choose the working regions for the parameters  $\mathbf{M}^2$  and  $\mathbf{s}_0$ . They should meet standard constraints of sum rule calculations, which have been discussed in Sec. II. For  $M_1^2$  and  $s_0$  which are actual for the  $T_{4c}$  channel, we employ the working regions Eq. (14). The parameters  $(M_2^2, s'_0)$  for the  $J/\psi$  channel are changed within limits

$$M_2^2 \in [4, 5] \text{ GeV}^2, \quad s'_0 \in [12, 13] \text{ GeV}^2. \quad (30)$$

In the second phase of analysis, we use

$$M_2^2 \in [4, 5] \text{ GeV}^2, \quad s'_0 \in [15, 16] \text{ GeV}^2. \quad (31)$$

The sum rule method gives reliable predictions in the deep-Euclidean region  $q^2 < 0$ . Therefore, it is convenient

to introduce a new variable  $Q^2 = -q^2$  and denote the obtained function by  $g_1(Q^2)$ . The range of  $Q^2$  analyzed by the sum rule method covers the interval  $Q^2 = 1 - 10 \text{ GeV}^2$ . Results of calculations are plotted in Fig. 5.

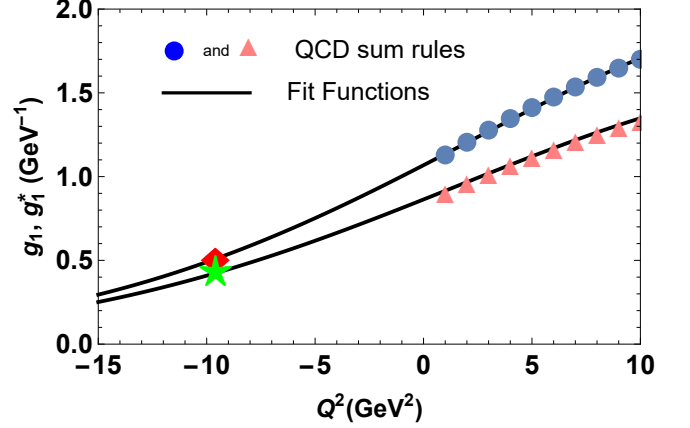


FIG. 5: The sum rule predictions and fit functions for the form factors  $g_1(Q^2)$  (upper line) and  $g_1^*(Q^2)$  (lower line). The red diamond and green star denote the point  $Q^2 = -m_1^2$ , where the strong couplings  $g_1$  and  $g_1^*$  are evaluated.

But the width of the decay  $T_{4c} \rightarrow J/\psi J/\psi$  is determined by the form factor  $g_1(q^2)$  at the mass shell  $q^2 = m_1^2$ . Stated differently, one has to find  $g_1(Q^2 = -m_1^2)$ . To avoid this problem, we use a fit function  $\mathcal{G}_1(Q^2)$ , which at momenta  $Q^2 > 0$  gives the same values as the sum rule calculations, but can be extrapolated to the region of  $Q^2 < 0$ . To this end, we employ functions  $\mathcal{G}_i^{(*)}(Q^2)$

$$\mathcal{G}_i^{(*)}(Q^2) = \mathcal{G}_i^{0(*)} \exp \left[ c_i^{1(*)} \frac{Q^2}{m^2} + c_i^{2(*)} \left( \frac{Q^2}{m^2} \right)^2 \right], \quad (32)$$

with parameters  $\mathcal{G}_i^{0(*)}$ ,  $c_i^{1(*)}$  and  $c_i^{2(*)}$ . Calculations demonstrate that  $\mathcal{G}_1^0 = 1.07 \text{ GeV}^{-1}$ ,  $c_1^1 = 2.99$ , and  $c_1^2 = -3.57$  give a nice agreement with the sum rules data for  $g_1(Q^2)$  shown in Fig. 5.

At the mass shell  $q^2 = m_1^2$  the function  $\mathcal{G}_1(Q^2)$  is equal to

$$g_1 \equiv \mathcal{G}_1(-m_1^2) = (5.1 \pm 1.1) \times 10^{-1} \text{ GeV}^{-1}. \quad (33)$$

Partial width of the process  $T_{4c} \rightarrow J/\psi J/\psi$  can be evaluated by employing the following expression

$$\Gamma[T_{4c} \rightarrow J/\psi J/\psi] = g_1^2 \frac{\lambda_1}{8\pi} \left( \frac{m_1^4}{m^2} + \frac{2\lambda_1^2}{3} \right), \quad (34)$$

where  $\lambda_1 = \lambda(m, m_1, m_1)$  and

$$\lambda(a, b, c) = \frac{\sqrt{a^4 + b^4 + c^4 - 2(a^2b^2 + a^2c^2 + b^2c^2)}}{2a}. \quad (35)$$

Then it is easy to find that

$$\Gamma[T_{4c} \rightarrow J/\psi J/\psi] = (56 \pm 18) \text{ MeV}. \quad (36)$$



The decay  $T_{4c} \rightarrow J/\psi\psi'$  can be explored in accordance with a scheme described above. In this case, the extrapolating function  $\mathcal{G}_1^*(Q^2)$  has the parameters  $\mathcal{G}_1^{0*} = 0.86 \text{ GeV}^{-1}$ ,  $c_1^* = 2.86$ , and  $c_1^{2*} = -3.47$ . The sum rule predictions for the form factor  $g_1^*(q^2)$ , as well as the function  $\mathcal{G}_1^*(Q^2)$  are depicted in Fig. 5. One can be convinced in a reasonable agreement between the sum rules data and  $\mathcal{G}_1^*(Q^2)$ .

The strong coupling  $g_1^*$  is calculated at the mass shell  $q^2 = m_1^2$

$$g_1^* \equiv \mathcal{G}_1^*(-m_1^2) = (4.2 \pm 1.0) \times 10^{-1} \text{ GeV}^{-1}. \quad (37)$$

The width of the process is found by means of Eq. (34) with the following substitutions  $g_1 \rightarrow g_1^*$ ,  $\lambda_1 \rightarrow \lambda_2 = \lambda(m, m_1^*, m_1)$ , and  $m_1^4 \rightarrow m_1^2 m_1^{*2}$  which leads to the result

$$\Gamma [T_{4c} \rightarrow J/\psi\psi'] = (15 \pm 5) \text{ MeV}. \quad (38)$$

Essential parameters of these decays are shown in Table II.

#### IV. PROCESSES $T_{4c} \rightarrow \eta_c \eta_c$ , $\eta_c \eta_c(2S)$

The decays  $T_{4c} \rightarrow \eta_c \eta_c$  and  $T_{4c} \rightarrow \eta_c \eta_c(2S)$  can be explored in a similar way. The strong couplings  $g_2$  and  $g_2^*$  which correspond to the vertices  $T_{4c} \eta_c \eta_c$  and  $T_{4c} \eta_c \eta_c(2S)$  can be extracted from the correlation function

$$\begin{aligned} \Pi(p, p') &= i^2 \int d^4x d^4y e^{ip'y} e^{-ipx} \langle 0 | \mathcal{T} \{ J^{\eta_c}(y) \\ &\times J^{\eta_c}(0) J^\dagger(x) \} | 0 \rangle, \end{aligned} \quad (39)$$

where the current  $J^{\eta_c}(x)$  is

$$J^{\eta_c}(x) = \bar{c}_i(x) i \gamma_5 c_i(x). \quad (40)$$

Separating the ground-level and first excited state contributions from effects of higher resonances and continuum states, we write the correlation function (39) in the following form

$$\begin{aligned} \Pi^{\text{Phys}}(p, p') &= \frac{\langle 0 | J^{\eta_c} | \eta_c(p') \rangle \langle 0 | J^{\eta_c} | \eta_c(q) \rangle}{p'^2 - m_2^2} \frac{\langle 0 | J^{\eta_c} | \eta_c(q) \rangle}{q^2 - m_2^2} \\ &\times \langle \eta_c(p') \eta_c(q) | T_{4c}(p) \rangle \frac{\langle T_{4c}(p) | J^\dagger | 0 \rangle}{p^2 - m^2} \\ &+ \frac{\langle 0 | J^{\eta_c} | \eta_c(2S)(p') \rangle \langle 0 | J^{\eta_c} | \eta_c(q) \rangle}{p'^2 - m_2^{*2}} \frac{\langle 0 | J^{\eta_c} | \eta_c(q) \rangle}{q^2 - m_2^2} \\ &\times \langle \eta_c(2S)(p') \eta_c(q) | T_{4c}(p) \rangle \frac{\langle T_{4c}(p) | J^\dagger | 0 \rangle}{p^2 - m^2} + \dots, \end{aligned} \quad (41)$$

where  $m_2$  and  $m_2^*$  are the masses of the  $\eta_c$  and  $\eta_c(2S)$  mesons. The matrix elements of scalar and two pseudoscalar particles' vertices are modeled in the form

$$\begin{aligned} \langle \eta_c(p') \eta_c(q) | T_{4c}(p) \rangle &= g_2(q^2) p \cdot p', \\ \langle \eta_c(2S)(p') \eta_c(q) | T_{4c}(p) \rangle &= g_2^*(q^2) p \cdot p'. \end{aligned} \quad (42)$$

To express the correlator  $\Pi^{\text{Phys}}(p, p')$  in terms of physical parameters of the particles  $T_{4c}$ ,  $\eta_c$ , and  $\eta_c(2S)$ , we use the matrix element Eq. (4) and

$$\langle 0 | J^{\eta_c} | \eta_c \rangle = \frac{f_2 m_2^2}{2m_c}, \quad \langle 0 | J^{\eta_c} | \eta_c(2S) \rangle = \frac{f_2^* m_2^{*2}}{2m_c}, \quad (43)$$

with  $f_2$  and  $f_2^*$  being the decay constants of the mesons  $\eta_c$  and  $\eta_c(2S)$ , respectively. The correlation function  $\Pi^{\text{Phys}}(p, p')$  then takes the form

$$\begin{aligned} \Pi^{\text{Phys}}(p, p') &= \frac{g_2(q^2) f m f_2^2 m_2^4}{8m_c^2 (p^2 - m^2) (p'^2 - m_2^2)} \\ &\times \frac{m^2 + m_2^2 - q^2}{q^2 - m_2^2} + \frac{g_2^*(q^2) f m f_2 m_2^2 f_2^* m_2^{*2}}{8m_c^2 (p^2 - m^2) (p'^2 - m_2^{*2})} \\ &\times \frac{m^2 + m_2^{*2} - q^2}{q^2 - m_2^2} + \dots. \end{aligned} \quad (44)$$

The correlation function  $\Pi^{\text{Phys}}(p, p')$  has simple Lorentz structure proportional to  $\mathbf{I}$ , hence right-hand side of Eq. (44) is the corresponding invariant amplitude  $\tilde{\Pi}^{\text{Phys}}(p^2, p'^2, q^2)$ .

Using quark-gluon degrees of freedom, we can find the QCD side of the sum rule

$$\begin{aligned} \Pi^{\text{OPE}}(p, p') &= 2i^2 \int d^4x d^4y e^{ip'y} e^{-ipx} \\ &\left\{ \times \text{Tr} \left[ \gamma_5 S_c^{ia}(y-x) \tilde{S}_c^{jb}(-x) \gamma_5 \tilde{S}_c^{bj}(x) S_c^{ai}(x-y) \right] \right. \\ &\left. + \text{Tr} \left[ \gamma_5 S_c^{ib}(y-x) \tilde{S}_c^{ja}(-x) \gamma_5 \tilde{S}_c^{bj}(x) S_c^{ai}(x-y) \right] \right\}. \end{aligned} \quad (45)$$

The sum rule for the strong form factor  $g_2(q^2)$  reads

$$\begin{aligned} g_2(q^2) &= \frac{8m_c^2}{f m f_2^2 m_2^4} \frac{q^2 - m_2^2}{m^2 + m_2^2 - q^2} \\ &\times e^{m^2/M_1^2} e^{m_2^2/M_2^2} \tilde{\Pi}(\mathbf{M}^2, \mathbf{s}_0, q^2), \end{aligned} \quad (46)$$

with  $\tilde{\Pi}(\mathbf{M}^2, \mathbf{s}_0, q^2)$  being the invariant amplitude  $\tilde{\Pi}^{\text{OPE}}(p^2, p'^2, q^2)$  corresponding to the correlator  $\Pi^{\text{OPE}}(p, p')$  after the Borel transformations and subtractions. Numerical computations are carried out using Eq. (46), parameters of the meson  $\eta_c$  from Table I, and working regions for  $\mathbf{M}^2$  and  $\mathbf{s}_0$ . The Borel and continuum subtraction parameters  $M_1^2$  and  $s_0$  in the  $T_{4c}$  channel are chosen as in Eq. (14), whereas for  $M_2^2$  and  $s'_0$  which correspond to the  $\eta_c$  channel, we employ

$$M_2^2 \in [3.5, 4.5] \text{ GeV}^2, \quad s'_0 \in [11, 12] \text{ GeV}^2. \quad (47)$$

The interpolating function  $\mathcal{G}_2(Q^2)$  has the following parameters:  $\mathcal{G}_2^0 = 0.38 \text{ GeV}^{-1}$ ,  $c_2^1 = 3.62$ , and  $c_2^2 = -4.17$ . For the strong coupling  $g_2$ , we get

$$g_2 \equiv \mathcal{G}_2(-m_2^2) = (1.7 \pm 0.4) \times 10^{-1} \text{ GeV}^{-1}. \quad (48)$$

The width of the process  $T_{4c} \rightarrow \eta_c \eta_c$  is determined by means of the formula

$$\Gamma [T_{4c} \rightarrow \eta_c \eta_c] = g_2^2 \frac{m_2^2 \lambda_2}{8\pi} \left( 1 + \frac{\lambda_2^2}{m_2^2} \right), \quad (49)$$



where  $\lambda_2 = \lambda(m, m_2, m_2)$ . Finally, we obtain

$$\Gamma [T_{4c} \rightarrow \eta_c \eta_c] = (24 \pm 8) \text{ MeV}. \quad (50)$$

For the channel  $T_{4c} \rightarrow \eta_c \eta_c(2S)$ , we use

$$M_2^* \in [3.5, 4.5] \text{ GeV}^2, \quad s_0^{*f} \in [13, 14] \text{ GeV}^2, \quad (51)$$

and find

$$g_2^* \equiv \mathcal{G}_2^*(-m_2^2) = (9.0 \pm 2.8) \times 10^{-2} \text{ GeV}^{-1}. \quad (52)$$

The  $g_2^*$  is evaluated using the fit function  $\mathcal{G}_2^*(Q^2)$  with the parameters  $\mathcal{G}_2^{0*} = 0.21 \text{ GeV}^{-1}$ ,  $c_2^{1*} = 3.62$ , and  $c_2^{2*} = -4.17$ . The width of this decay is equal to

$$\Gamma [T_{4c} \rightarrow \eta_c \eta_c(2S)] = (5 \pm 2) \text{ MeV}. \quad (53)$$

## V. DECAYS $T_{4c} \rightarrow \eta_c \chi_{c1}(1P)$ AND $T_{4c} \rightarrow \chi_{c0} \chi_{c0}$

In this section, we study the processes  $T_{4c} \rightarrow \eta_c \chi_{c1}(1P)$  and  $T_{4c} \rightarrow \chi_{c0} \chi_{c0}$ , which are the  $P$ - and  $S$ -wave decays of the tetraquark  $T_{4c}$ , respectively. The two-meson thresholds for these decay channels are equal to 6495 MeV and 6830 MeV, hence they are kinematically allowed modes of  $T_{4c}$ .

### A. $T_{4c} \rightarrow \eta_c \chi_{c1}(P)$

Treatment of the  $P$ -wave process  $T_{4c} \rightarrow \eta_c \chi_{c1}(P)$  is performed in the context of the standard method. The three-point correlator to be considered in this case is

$$\begin{aligned} \Pi_\mu(p, p') &= i^2 \int d^4x d^4y e^{ip'y} e^{-ipx} \langle 0 | \mathcal{T} \{ J_\mu^{\chi_{c1}}(y) \\ &\times J^{\eta_c}(0) J^\dagger(x) \} | 0 \rangle, \end{aligned} \quad (54)$$

where  $J_\mu^{\chi_{c1}}(y)$  is the interpolating current for the meson  $\chi_{c1}(1P)$

$$J_\mu^{\chi_{c1}}(y) = \bar{c}_j(x) \gamma_5 \gamma_\mu c_j(y). \quad (55)$$

In terms of the physical parameters of involved particles the correlation function has the form

$$\begin{aligned} \Pi_\mu^{\text{Phys}}(p, p') &= g_3(q^2) \frac{f m f_2 m_2^2 f_3 m_3}{2m_c(p^2 - m^2)(p'^2 - m_3^2)} \\ &\times \frac{1}{q^2 - m_2^2} \left[ \frac{m^2 - m_3^2 - q^2}{2m_3^2} p'_\mu - q_\mu \right] + \dots \end{aligned} \quad (56)$$

In Eq. (56)  $m_3$  and  $f_3$  are the mass and decay constant of the meson  $\chi_{c1}(1P)$ , respectively. To derive the correlator  $\Pi_\mu^{\text{Phys}}(p, p')$ , we have used the known matrix elements of the tetraquark  $T_{4c}$  and meson  $\eta_c$ , as well as new matrix elements

$$\langle 0 | J_\mu^{\chi_{c1}} | \chi_{c1}(p') \rangle = f_3 m_3 \varepsilon_\mu^*(p'), \quad (57)$$

and

$$\langle \eta_c(q) \chi_{c1}(p') | T_{4c}(p) \rangle = g_3(q^2) p \cdot \varepsilon^*(p'), \quad (58)$$

where  $\varepsilon_\mu^*(p')$  is the polarization vector of  $\chi_{c1}(1P)$ .

The QCD side  $\Pi_\mu^{\text{OPE}}(p, p')$  is given by the formula

$$\begin{aligned} \Pi_\mu^{\text{OPE}}(p, p') &= 2i \int d^4x d^4y e^{ip'y} e^{-ipx} \\ &\times \left\{ \text{Tr} \left[ \gamma_\mu \gamma_5 S_c^{ia}(y-x) \tilde{S}_c^{jb}(-x) \gamma_5 \tilde{S}_c^{bj}(x) S_c^{ai}(x-y) \right] \right. \\ &\left. + \text{Tr} \left[ \gamma_\mu \gamma_5 S_c^{ib}(y-x) \tilde{S}_c^{ja}(-x) \gamma_5 \tilde{S}_c^{bj}(x) S_c^{ai}(x-y) \right] \right\}. \end{aligned} \quad (59)$$

The sum rule for  $g_3(q^2)$  is derived using invariant amplitudes corresponding to terms  $\sim p'_\mu$  in  $\Pi_\mu^{\text{Phys}}(p, p')$  and  $\Pi_\mu^{\text{OPE}}(p, p')$ .

In numerical analysis, the parameters  $M_2^*$  and  $s_0'$  in the  $\chi_{c1}$  channel are chosen in the following way

$$M_2^* \in [4, 5] \text{ GeV}^2, \quad s_0' \in [13, 14] \text{ GeV}^2. \quad (60)$$

For the parameters of the fit function  $\mathcal{G}_3(Q^2)$ , we get  $\mathcal{G}_3^0 = 5.16$ ,  $c_3^1 = 3.16$ , and  $c_3^2 = -3.87$ . Then, the strong coupling  $g_3$  is equal to

$$g_3 \equiv \mathcal{G}_3(-m_2^2) = 2.5 \pm 0.6. \quad (61)$$

The width of the decay  $T_{4c} \rightarrow \eta_c \chi_{c1}(P)$  can be calculated by mean of the expression

$$\Gamma [T_{4c} \rightarrow \eta_c \chi_{c1}(P)] = g_3^2 \frac{\lambda_3^3}{24\pi m_3^2}, \quad (62)$$

where  $\lambda_3 = \lambda(m, m_3, m_2)$ . The width of this process is equal to

$$\Gamma [T_{4c} \rightarrow \eta_c \chi_{c1}(P)] = (12 \pm 4) \text{ MeV}. \quad (63)$$

### B. $T_{4c} \rightarrow \chi_{c0} \chi_{c0}$

To explore the decay  $T_{4c} \rightarrow \chi_{c0} \chi_{c0}$ , we consider the correlation function

$$\begin{aligned} \Pi(p, p') &= i^2 \int d^4x d^4y e^{ip'y} e^{-ipx} \langle 0 | \mathcal{T} \{ J^{\chi_{c0}}(y) \\ &\times J^{\chi_{c0}}(0) J^\dagger(x) \} | 0 \rangle, \end{aligned} \quad (64)$$

with  $J^{\chi_{c0}}(x)$  being the interpolating current for the scalar meson  $\chi_{c0}$

$$J^{\chi_{c0}}(x) = \bar{c}_i(x) c_i(x). \quad (65)$$

The physical side  $\Pi^{\text{Phys}}(p, p')$  of the sum rule is

$$\begin{aligned} \Pi^{\text{Phys}}(p, p') &= g_4(q^2) \frac{f m f_4 m_4}{2(p^2 - m^2)(p'^2 - m_4^2)} \\ &\times \frac{m^2 + m_4^2 - q^2}{q^2 - m_4^2} + \dots, \end{aligned} \quad (66)$$

$i$	Channels	$g_i^{(*)} \times 10$ (GeV $^{-1}$ )	$\Gamma_i^{(*)}$ (MeV)
1	$T_{4c} \rightarrow J/\psi J/\psi$	$5.1 \pm 1.1$	$56 \pm 18$
1*	$T_{4c} \rightarrow J/\psi \psi'$	$4.2 \pm 1.0$	$15 \pm 5$
2	$T_{4c} \rightarrow \eta_c \eta_c$	$1.7 \pm 0.4$	$24 \pm 8$
2*	$T_{4c} \rightarrow \eta_c \eta_c (2S)$	$0.9 \pm 0.28$	$5 \pm 2$
3	$T_{4c} \rightarrow \eta_c \chi_{c1} (1P)$	$25 \pm 6^*$	$12 \pm 4$
4	$T_{4c} \rightarrow \chi_{c0} \chi_{c0}$	$2.4 \pm 0.45$	$16 \pm 5$
5	$T_{4b} \rightarrow \eta_b \eta_b$	$1.9 \pm 0.4$	$94 \pm 28$

TABLE II: Decay channels of the tetraquarks  $T_{4c}$  and  $T_{4b}$ , strong couplings  $g_i^{(*)}$ , and partial widths  $\Gamma_i^{(*)}$ . The coupling  $g_3$  is dimensionless.

where  $m_4$  and  $f_4$  are the mass and decay constant of the meson  $\chi_{c0}$ . The correlator  $\Pi^{\text{OPE}}(p, p')$  has the form

$$\begin{aligned} \Pi^{\text{OPE}}(p, p') &= 2 \int d^4x d^4y e^{ip'y} e^{-ipx} \\ &\times \left\{ \text{Tr} \left[ S_c^{ia}(y-x) \tilde{S}_c^{jb}(-x) \tilde{S}_c^{bj}(x) S_c^{ai}(x-y) \right] \right. \\ &\left. + \text{Tr} \left[ S_c^{ib}(y-x) \tilde{S}_c^{ja}(-x) \tilde{S}_c^{bj}(x) S_c^{ai}(x-y) \right] \right\}. \end{aligned} \quad (67)$$

The following operations are performed in the context of the standard approach.

In numerical computations, the parameters  $M_2^2$  and  $s'_0$  in the  $\chi_{c0}$  channel are chosen in the form

$$M_2^2 \in [4, 5] \text{ GeV}^2, \quad s'_0 \in [14, 14.9] \text{ GeV}^2, \quad (68)$$

where  $s'_0$  is limited by the mass of the charmonium  $\chi_{c0}(3860)$ . The coupling  $g_4$  which corresponds to the vertex  $T_{4c} \chi_{c0} \chi_{c0}$  is extracted at  $Q^2 = -m_4^2$  of the fit function  $\mathcal{G}_4(Q^2)$  with parameters  $\mathcal{G}_4^0 = 0.56$ ,  $c_4^1 = 2.81$ , and  $c_4^2 = -2.98$ .

The strong coupling  $g_4$  equals to

$$g_4 \equiv \mathcal{G}_4(-m_4^2) = (2.4 \pm 0.45) \times 10^{-1} \text{ GeV}^{-1}. \quad (69)$$

The partial width of the decay  $T_{4c} \rightarrow \chi_{c0} \chi_{c0}$  is computed by employing the expression

$$\Gamma [T_{4c} \rightarrow \chi_{c0} \chi_{c0}] = g_4^2 \frac{m_4^2 \lambda_4}{8\pi} \left( 1 + \frac{\lambda_4^2}{m_4^2} \right), \quad (70)$$

where  $\lambda_4 = \lambda(m, m_4, m_4)$ . Numerical analyses lead to the result

$$\Gamma [T_{4c} \rightarrow \chi_{c0} \chi_{c0}] = (16 \pm 5) \text{ MeV}. \quad (71)$$

The partial widths of six decays of the tetraquark  $T_{4c}$  are collected in Table II. Using these predictions, it is easy to find that

$$\Gamma_{4c} = (128 \pm 22) \text{ MeV}. \quad (72)$$

## VI. WIDTH OF THE TETRAQUARK $T_{4b}$

In this section, we evaluate the width of the fully heavy tetraquark  $T_{4b}$ . Our analysis shows that  $T_{4b}$  can dissociate to mesons  $\eta_b \eta_b$ . Investigation of the decay  $T_{4b} \rightarrow \eta_b \eta_b$  can be performed in accordance with a scheme utilized in the section IV while considering the process  $T_{4c} \rightarrow \eta_c \eta_c$ .

The correlation function necessary to extract a sum rule for the form factor  $g_4(q^2)$  in this case is given by the expression

$$\begin{aligned} \Pi_b(p, p') &= i^2 \int d^4x d^4y e^{ip'y} e^{-ipx} \langle 0 | \mathcal{T} \{ J^{\eta_b}(y) \\ &\times J^{\eta_b}(0) J^\dagger(x) \} | 0 \rangle, \end{aligned} \quad (73)$$

where  $J^{\eta_b}(x)$  in the interpolating current for the meson  $\eta_b$

$$J^{\eta_b}(x) = \bar{b}_j(x) i\gamma_5 b_j(x). \quad (74)$$

To determine  $g_5$ , we use the standard "ground-state+continuum" scheme. Then, it is not difficult to find the physical side of the sum rule, which is given by the following expression

$$\begin{aligned} \Pi_b^{\text{Phys}}(p, p') &= \frac{\langle 0 | J^{\eta_b} | \eta_b(p') \rangle \langle 0 | J^{\eta_b} | \eta_b(q) \rangle}{p'^2 - m_5^2} \frac{\langle 0 | J^{\eta_b} | \eta_b(q) \rangle}{q^2 - m_5^2} \\ &\times \langle \eta_b(p') \eta_b(q) | T_{4b}(p) \rangle \frac{\langle T_{4b}(p) | J^\dagger | 0 \rangle}{p^2 - m^2} + \dots, \end{aligned} \quad (75)$$

where  $m_5$  is the mass of the  $\eta_b$  meson. The matrix elements which are required to simplify  $\Pi_b^{\text{Phys}}(p, p')$  have the forms

$$\begin{aligned} \langle 0 | J^{\eta_b} | \eta_b \rangle &= \frac{f_5 m_5^2}{2m_b}, \\ \langle \eta_b(p') \eta_b(q) | T_{4b}(p) \rangle &= g_5(q^2) p \cdot p, \end{aligned} \quad (76)$$

where  $f_5$  is the decay constant of  $\eta_b$ .

To find the QCD side of the sum rule  $\Pi^{\text{OPE}}(p, p')$  one needs to replace all  $c$ -quark propagators in Eq. (45) by relevant  $S_b(x)$  propagators. The sum rule for the coupling predicts

$$g_5 \equiv \mathcal{G}_5(-m_5^2) = (1.9 \pm 0.4) \times 10^{-1} \text{ GeV}^{-1}. \quad (77)$$

The coupling  $g_5$  is calculated by means of the extrapolating function  $\mathcal{G}_5(Q^2)$  with  $\mathcal{G}_5^0 = 0.63$ ,  $c_5^1 = 3.21$ , and  $c_5^2 = -6.58$ . In sum rule computations the parameters  $M_1^2$  and  $s_0$  in  $T_{4b}$  channel are chosen in accordance with Eq. (16), whereas for  $M_2^2$  and  $s'_0$  in the  $\eta_b$  channel, we employ

$$M_2^2 \in [10, 12] \text{ GeV}^2, \quad s'_0 \in [93, 97] \text{ GeV}^2. \quad (78)$$

Results obtained for  $g_5(Q^2)$  and the function  $\mathcal{G}_5(Q^2)$  are plotted in Fig. 6.

The width of the decay  $T_{4b} \rightarrow \eta_b \eta_b$  can be found by means of the expression Eq. (49) with evident substitutions. Our prediction reads

$$\Gamma [T_{4b} \rightarrow \eta_b \eta_b] = (94 \pm 28) \text{ MeV}. \quad (79)$$

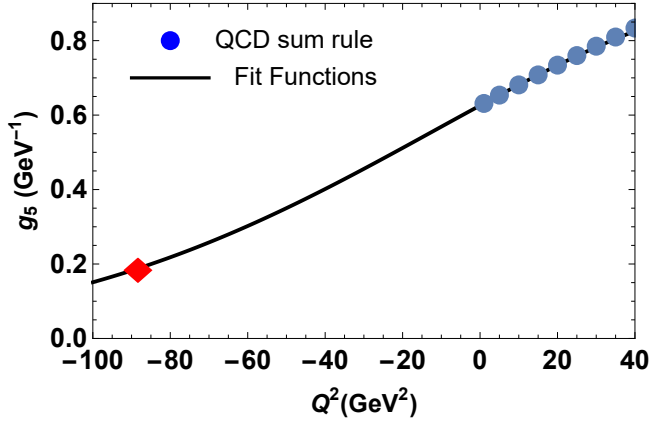


FIG. 6: The sum rule predictions and fit function for the strong coupling  $g_5(Q^2)$ .

## VII. DISCUSSION AND CONCLUDING NOTES

We have explored the fully charmed and beauty tetraquarks  $T_{4c}$  and  $T_{4b}$  in the context of QCD sum rule method. We have modeled them as diquark-antidiquark systems composed of  ${}^3P_0$  pseudoscalar states  $Q^T C Q$  and  $\overline{Q} C \overline{Q}^T$  with quantum numbers  $J^P = 0^-$ . Our present investigations include detailed calculations of both the mass and width of these tetraquarks.

Predictions obtained for the mass and full width of  $T_{4c}$

$$\begin{aligned} m &= (6928 \pm 50) \text{ MeV} \\ \Gamma_{4c} &= (128 \pm 22) \text{ MeV}. \end{aligned} \quad (80)$$

allow us to confront them with the available data of the LHCb-ATLAS-CMS Collaborations. The data of interest, reported by these experiments are

$$\begin{aligned} m^{\text{LHCb}} &= (6905 \pm 11 \pm 7) \text{ MeV}, \\ \Gamma^{\text{LHCb}} &= (80 \pm 19 \pm 33) \text{ MeV}, \end{aligned} \quad (81)$$

$$\begin{aligned} m^{\text{ATL}} &= 6870 \pm 30_{-10}^{+60} \text{ MeV}, \\ \Gamma^{\text{ATL}} &= 120 \pm 40_{-10}^{+30} \text{ MeV}, \end{aligned} \quad (82)$$

and

$$\begin{aligned} m^{\text{CMS}} &= (6927 \pm 9 \pm 5) \text{ MeV}, \\ \Gamma^{\text{CMS}} &= (122 \pm 22 \pm 19) \text{ MeV}, \end{aligned} \quad (83)$$

respectively. It is evident that  $m$  and  $\Gamma_{4c}$  are in excellent agreements with  $m^{\text{CMS}}$  and  $\Gamma^{\text{CMS}}$  of the CMS Collaboration. Within errors of calculations, they are also compatible with data of other experiments. Therefore, by taking into account these circumstances, we are inclined to idea that this tetraquark is nice candidate to the resonance  $X(6900)$ . Our conclusions about the nature of  $X(6900)$  are in accord with those of Ref. [24].

In Ref. [35], we performed an analysis for the fully charmed scalar diquark-antidiquark state  $X_{4c}$  built of  ${}^3S_1$  states  $Q^T C \gamma_\mu Q$  and  $\overline{Q} \gamma_\mu C \overline{Q}^T$  with spin-parity  $J^P = 1^+$ . It is known, that different diquark-antidiquark currents can be expressed in terms of molecular-type currents by means of the Fierz transformations [48, 49]. Contrary, a molecule current can be presented as a weighted sum of different diquark-antidiquark ones [50]. By performing similar operations, it is possible to find some common pieces in the currents used in Ref. [35] and in the present work. However, four-quark systems composed of  ${}^3P_0$  or  ${}^3S_1$  diquarks have different inner organizations and parameters. For instance, the mass  $(6570 \pm 55)$  MeV of the tetraquark  $X_{4c}$  is considerably smaller than  $m$ , which allowed us to identify it in Ref. [35] with the resonance  $X(6600)$ .

The fully beauty exotic mesons during past years were also under intensive investigations. The tetraquark  $T_{4b}$  that has been studied in this article, is a beauty counterpart of the fully charmed state  $T_{4c}$ . It turned out that  $T_{4b}$  can decay to  $\eta_b \eta_b$  pairs and be detected in a mass distribution of these mesons. Its parameters may be interesting for future experimental studies of fully beauty resonances.

### Appendix: Heavy quark propagator $S_Q^{ab}(x)$ and spectral density $\rho^{\text{pert.}}(s, \alpha, \beta, \gamma)$

In this paper, we use for the heavy quark propagator  $S_Q^{ab}(x)$  ( $Q = c, b$ ) the following expression

$$\begin{aligned} S_Q^{ab}(x) &= i \int \frac{d^4 k}{(2\pi)^4} e^{-ikx} \left\{ \frac{\delta_{ab} (\not{k} + m_Q)}{k^2 - m_Q^2} - \frac{g_s G_{ab}^{\alpha\beta} \sigma_{\alpha\beta} (\not{k} + m_Q) + (\not{k} + m_Q) \sigma_{\alpha\beta}}{4 (k^2 - m_Q^2)^2} \right. \\ &\quad \left. + \frac{g_s^2 G^2}{12} \delta_{ab} m_Q \frac{k^2 + m_Q \not{k}}{(k^2 - m_Q^2)^4} + \dots \right\}, \end{aligned} \quad (A.1)$$

where the notations

$$G_{ab}^{\alpha\beta} \equiv G_A^{\alpha\beta} \lambda_{ab}^A / 2, \quad G^2 = G_{\alpha\beta}^A G_A^{\alpha\beta}, \quad (\text{A.2})$$

have been employed. Here,  $G_A^{\alpha\beta}$  is the gluon field-strength tensor, and  $\lambda^A$  are the Gell-Mann matrices. The indices  $A, B, C$  run in the range  $1, 2, \dots, 8$ .

The invariant amplitude  $\Pi(M^2, s_0)$  obtained after the Borel transformation and continuum subtraction has the form

$$\Pi(M^2, s_0) = \int_{16m_Q^2}^{s_0} ds \rho^{\text{OPE}}(s) e^{-s/M^2},$$

where the spectral density  $\rho^{\text{OPE}}(s)$  is determined by the formula

$$\rho^{\text{OPE}}(s) = \rho^{\text{pert.}}(s) + \langle \alpha_s G^2 / \pi \rangle \rho^{\text{Dim4}}(s).$$

The components  $\rho^{\text{pert.}}(s)$  and  $\rho^{\text{Dim4}}(s)$  of the spectral density are

$$\rho^{\text{pert.}(\text{Dim4})}(s) = \int_0^1 d\alpha \int_0^{1-\alpha} d\beta \int_0^{1-\alpha-\beta} d\gamma \rho^{\text{pert.}(\text{Dim4})}(s, \alpha, \beta, \gamma), \quad (\text{A.3})$$

with  $\alpha, \beta,$  and  $\gamma$  being the Feynman parameters.

The function  $\rho^{\text{pert.}}(s, \alpha, \beta, \gamma)$  is given by the formula

$$\begin{aligned} \rho^{\text{pert.}}(s, \alpha, \beta, \gamma) = & \frac{\Theta(L_3) N_1^2}{2048\pi^6 N_2^8 N_3^5 L_1^2} \{ 33N_1^2 (L\gamma N_3^2 L\gamma + N_3(-2\gamma^4 + \alpha^2 L_1(-2 + 3(\gamma + \beta) + 4\alpha) - L_1^2(\beta\gamma + \alpha(\beta + \gamma))) \\ & + \alpha(\gamma^4(\alpha + \beta) + \alpha L_2^2(\beta(\beta - 1) + \alpha(\beta - 1) + \alpha^2) + \gamma^3(3\beta(\beta - 1) + \alpha(5\beta - 3) + 3\alpha^2) + \gamma^2 L_2(3\beta(\beta - 1) \\ & + \alpha(5\beta - 3) + 4\alpha^2) + \gamma L_2(\beta(\beta - 1)^2 + \alpha + \alpha\beta(4\beta - 5) + \alpha^2(5\beta - 4) + 3\alpha^2))) + 6(11L^5 s^2 \gamma \alpha^5 (L\gamma\alpha - N_2)^3 \\ & + N_3 L^2 s \alpha^2 (L\gamma\alpha - N_2)^2 (22N_2 L^2 s \gamma \alpha^2 - 22L^3 s \gamma^2 \alpha^3 + N_2^2 m_Q^2 (L_1^2 + 11L_1\alpha - 11\alpha^2)) + N_2^2 N_3^3 m_Q^2 (11N_2^2 (m_Q^2 L_1^2 - Ls\alpha) \\ & - N_2 Ls\gamma\alpha (L_1^2 + 22L_1\alpha - 22\alpha^2) + L^2 s \gamma^2 \alpha^2 (L_1^2 + 11L_1\alpha - 11\alpha^2)) + N_3^2 Ls\alpha (L\gamma\alpha - N_2) (-22N_2 L^3 s \gamma^2 \alpha^3 + 11L^4 s \gamma^3 \alpha^4 \\ & + N_3^2 m_Q^2 (L_1^2 + 22L_1\alpha - 22\alpha^2) + N_2^2 L\gamma\alpha (11Ls\alpha + m_Q^2 (-13L_1^2 - 22L_1\alpha + 22\alpha^2))) - 2N_1 (2N_3^3 N_2^2 m_Q^2 (L_1^2 + 11L_1\alpha \\ & - 11\alpha^2) + N_3 (-132L^5 s \gamma^2 \alpha^5 + 33N_2 L^3 s \gamma \alpha^3 (L_1\gamma + 6\alpha(L_2 + \gamma)) + N_2^2 (-33L^2 s \alpha^2 (L_1\gamma + 2\alpha(L_2 + \gamma)) + 2m_Q^2 (L_1^2 \\ & + 11L_1\alpha - 11\alpha^2) (-\alpha^2 + L_1(\alpha + \beta)) (-\alpha^2 + L_1(\alpha + \gamma)))) + 33L^3 s \alpha^3 (2L^3 \alpha^3 \gamma^2 + N_2 (L_1\gamma + \alpha(L_2 + \gamma)) \\ & + N_2 \alpha \gamma (L_1^2 \gamma - \alpha(3L_2^2 + \gamma(-5 + 2\gamma + 5\beta + 6\alpha)))) + N_3^2 (-99N_2 L^3 s \gamma \alpha^3 + 66L^4 s \gamma^2 \alpha^4 + N_2^2 (33L^2 s \alpha^2 + 2m_Q^2 (22\alpha^4 \\ & - L_1 \alpha^2 (-9 + 20\gamma + 20\beta + 44\alpha) + L_1^2 (11\gamma\beta + 13\alpha - 2(\beta + \gamma)\alpha)))) \}. \end{aligned} \quad (\text{A.4})$$

In expression above,  $\Theta(z)$  is the Unit Step function. We have introduced also the following notations

$$\begin{aligned} N_1 = & s\alpha\beta\gamma [\gamma^3 + \alpha(\beta + \alpha - 1)^2 + \gamma(\beta + \alpha - 1)(-1 + 2\gamma + \alpha + 2\beta)] - m_Q^2 [\gamma^4(\beta + \alpha) + \alpha(\beta + \alpha - 1)^2 \\ & \times (2\gamma\beta + (\gamma + \beta)\alpha) + \gamma^2(\beta + \alpha - 1)(\beta^2 - \alpha + 2\alpha(\alpha + \gamma) + \beta(-1 + 2\gamma + \alpha + 4\beta))], \\ N_2 = & \beta\alpha(\alpha + \beta - 1) + \gamma^2(\alpha + \beta) + \gamma[\beta^2 + \alpha(\alpha - 1) + \beta(2\alpha - 1)], \quad N_3 = \gamma^2 + (\gamma + \alpha)(\beta + \alpha - 1), \\ L = & \alpha + \beta + \gamma - 1, \quad L_1 = 1 - \beta - \gamma, \quad L_2 = \alpha + \beta - 1, \quad L_3 = N_3 [s\alpha\beta\gamma L - m_Q^2 N_2] / N_2^2. \end{aligned} \quad (\text{A.5})$$

- 
- [1] R. L. Jaffe, *Multi-Quark Hadrons. 1. The Phenomenology of  $q^2\bar{q}^2$  Mesons*, Phys. Rev. D **15**, 267 (1977).  
[2] R. L. Jaffe, *Perhaps a Stable Dihyperon*, Phys. Rev. Lett. **38**, 195 (1977); **38**, 617(E) (1977).  
[3] J. P. Ader, J. M. Richard, and P. Taxil, *Do Narrow Heavy Multi - Quark States Exist?*, Phys. Rev. D **25**,

- 2370 (1982).  
[4] S. Zouzou, B. Silvestre-Brac, C. Gignoux, and J. M. Richard, *Four Quark Bound States*, Z. Phys. C **30**, 457 (1986).  
[5] H. J. Lipkin, *A Model Independent Approach To Multi - Quark Bound States*, Phys. Lett. B **172**, 242 (1986).

- [6] J. Carlson, L. Heller, and J. A. Tjon, *Stability of Dimesons*, Phys. Rev. D **37**, 744 (1988).
- [7] F. S. Navarra, M. Nielsen, and S. H. Lee, *QCD sum rules study of  $QQ\bar{u}\bar{d}$  mesons*, Phys. Lett. B **649**, 166 (2007).
- [8] E. J. Eichten and C. Quigg, *Heavy-quark symmetry implies stable heavy tetraquark mesons  $Q_i Q_j \bar{q}_k \bar{q}_l$* , Phys. Rev. Lett. **119**, 202002 (2017).
- [9] M. Karliner and J. L. Rosner, *Discovery of doubly-charmed  $\Xi_{cc}$  baryon implies a stable  $(bb\bar{u}\bar{d})$  tetraquark*, Phys. Rev. Lett. **119**, 202001 (2017).
- [10] Y. Xing and R. Zhu, *Weak decays of the stable doubly heavy tetraquark states*, Phys. Rev. D **98**, 053005 (2018).
- [11] S. S. Agaev, K. Azizi, B. Barsbay, and H. Sundu, *Weak decays of the axial-vector tetraquark  $T_{bb;\bar{u}\bar{d}}^-$* , Phys. Rev. D **99**, 033002 (2019).
- [12] G. Li, X. F. Wang and Y. Xing, *SU(3) analysis of weak decays of doubly-heavy tetraquarks  $b\bar{c}\bar{q}\bar{q}$* , Eur. Phys. J. C **79**, 210 (2019).
- [13] H. Sundu, S. S. Agaev, and K. Azizi, *Semileptonic decays of the scalar tetraquark  $Z_{bc;\bar{u}\bar{d}}^0$* , Eur. Phys. J. C **79**, 753 (2019).
- [14] S. S. Agaev, K. Azizi, and H. Sundu, *Double-heavy axial-vector tetraquark  $T_{bc;\bar{u}\bar{d}}^0$* , Nucl. Phys. B **951**, 114890 (2020).
- [15] S. S. Agaev, K. Azizi, B. Barsbay, and H. Sundu, *Heavy exotic scalar meson  $T_{bb;\bar{u}\bar{s}}^-$* , Phys. Rev. D **101**, 094026 (2020).
- [16] S. S. Agaev, K. Azizi, B. Barsbay, and H. Sundu, *Stable scalar tetraquark  $T_{bb;\bar{u}\bar{d}}^-$* , Eur. Phys. J. A **56**, 177 (2020).
- [17] S. S. Agaev, K. Azizi, B. Barsbay, and H. Sundu, *Semileptonic and nonleptonic decays of the axial-vector tetraquark  $T_{bb;\bar{u}\bar{d}}^-$* , Eur. Phys. J. A **57**, 106 (2021).
- [18] S. S. Agaev, K. Azizi, B. Barsbay, and H. Sundu, *A family of double-beauty tetraquarks: Axial-vector state  $T_{bb;\bar{u}\bar{s}}^-$* , Chin. Phys. C **45**, 013105 (2021).
- [19] F. S. Yu, *Weak-decay searches for  $Qs\bar{u}\bar{d}$* , Eur. Phys. J. C **82**, 641 (2022).
- [20] R. Aaij *et al.* (LHCb Collaboration), *Observation of structure in the  $J/\psi$ -pair mass spectrum*, Sci. Bull. **65**, 1983 (2020).
- [21] E. Bouhova-Thacker (ATLAS Collaboration), *ATLAS results on exotic hadronic resonances*, PoS **ICHEP2022**, 806 (2022).
- [22] A. Hayrapetyan, *et al.* (CMS Collaboration), *Recent CMS results on exotic resonances*, arXiv:2306.07164 [hep-ex].
- [23] J. R. Zhang,  *$0^+$  fully-charmed tetraquark states*, Phys. Rev. D **103**, 014018 (2021).
- [24] R. M. Albuquerque, S. Narison, A. Rabemananjara, D. Rabetiariyony, and G. Randriamanatrika, *Doubly-hidden scalar heavy molecules and tetraquarks states from QCD at NLO*, Phys. Rev. D **102**, 094001 (2020).
- [25] Z. G. Wang, *Analysis of the  $X(6600)$ ,  $X(6600)$ ,  $X(7300)$  and related tetraquark states with the QCD sum rules*, Nucl. Phys. B **985**, 115983 (2022).
- [26] W. C. Dong and Z. G. Wang, *Going in quest of potential tetraquark interpretations for the newly observed  $T_{\psi\psi}$  states in light of the diquark-antidiquark scenarios*, Phys. Rev. D **107**, 074010 (2023).
- [27] R. N. Faustov, V. O. Galkin, and E. M. Savchenko, *Fully-heavy tetraquark spectroscopy in the relativistic quark model*, Symmetry **14**, 2504 (2022).
- [28] Y. Lu, C. Cheng, K. G. Kang, G. y. Qin, and H. Q. Zheng,  *$X(6900)$  peak could be a molecular state*, Phys. Rev. D **107**, 094006 (2023).
- [29] X. K. Dong, V. Baru, F. K. Guo, C. Hanhart, and A. Nefediev, *Coupled-Channel Interpretation of the LHCb Double- $J/\psi$  Spectrum and Hints of a New State Near the  $J/\psi J/\psi$  Threshold*, Phys. Rev. Lett. **126**, 132001 (2021); **127**, 119901(E) (2021).
- [30] Z. R. Liang, X. Y. Wu, and D. L. Yao, *Hunting for states in the recent LHCb di- $J/\psi$  invariant mass spectrum*, Phys. Rev. D **104**, 034034 (2021).
- [31] C. Gong, M. C. Du, Q. Zhao, X. H. Zhong, and B. Zhou *Nature of  $X(6900)$  and its production mechanism at LHCb*, Phys. Lett. B **824**, 136794 (2022).
- [32] P. Niu, Z. Zhang, Q. Wang, and M. L. Du, *The third peak structure in the double  $J/\psi$  spectrum*, arXiv:2212.06535.
- [33] G. L. Yu, Z. Y. Li, Z. G. Wang, J. Lu, and M. Yan, *The  $S$  and  $P$  wave fully charmed tetraquark states and their radial excitations*, Eur. Phys. J. C **83**, 416 (2023).
- [34] S. Q. Kuang, Q. Zhou, D. Guo, Q. H. Yang, and L. Y. Dai, *Study of  $X(6900)$  with unitarized coupled channel scattering amplitudes*, Eur. Phys. J. C **83**, 383 (2023).
- [35] S. S. Agaev, K. Azizi, B. Barsbay, and H. Sundu, Phys. Lett. B **844**, 138089 (2023).
- [36] C. Becchi, A. Giachino, L. Maiani, and E. Santopinto, *Search for  $bb\bar{b}\bar{b}$  tetraquark decays in 4 muons,  $B^+B^-$ ,  $B^0\bar{B}^0$  and  $B_s^0\bar{B}_s^0$  channels at LHC*, Phys. Lett. B **806**, 135495 (2020).
- [37] C. Becchi, A. Giachino, L. Maiani, and E. Santopinto, *A study of  $cc\bar{c}\bar{c}$  tetraquark decays in 4 muons and in  $D^{(*)}\bar{D}^{(*)}$  at LHCb*, Phys. Lett. B **811**, 135952 (2020).
- [38] M. A. Shifman, A. I. Vainshtein and V. I. Zakharov, *QCD and Resonance Physics. Theoretical Foundations*, Nucl. Phys. B **147**, 385 (1979).
- [39] M. A. Shifman, A. I. Vainshtein and V. I. Zakharov, *QCD and Resonance Physics: Applications*, Nucl. Phys. B **147**, 448 (1979).
- [40] S. S. Agaev, K. Azizi, and H. Sundu, *Four-quark exotic mesons*, Turk. J. Phys. **44**, 95 (2020).
- [41] R. L. Workman *et al.* (Particle Data Group), *Prog. Theor. Exp. Phys.* **2022**, 083C01 (2022).
- [42] T. Barnes, S. Godfrey, and E. S. Swanson, *Higher charmonia*, Phys. Rev. D **72**, 054026 (2005).
- [43] V. V. Kiselev, A. K. Likhoded, O. N. Pakhomova, and V. A. Saleev, *Leptonic constants of heavy quarkonia in potential approach of NRQCD*, Phys. Rev. D **65**, 034013 (2002).
- [44] D. Hatton *et al.* (HPQCD Collaboration), *Charmonium properties from lattice QCD+QED: hyperfine splitting,  $J/\psi$  leptonic width, charm quark mass and  $a_\mu^c$* , Phys. Rev. D **102**, 054511 (2020).
- [45] D. Hatton, C. T. H. Davies, J. Koponen, G. P. Lepage, and A. T. Lytle, *Bottomonium precision tests from full lattice QCD: hyperfine splitting,  $\Upsilon$  leptonic width and  $b$  quark contribution to  $e^+e^- \rightarrow$  hadrons*, Phys. Rev. D **103**, 054512 (2021).
- [46] E. Veli Veliev, K. Azizi, H. Sundu, and G. Kaya, *Spectrum of the heavy axial-vector  $\chi_{b1}(1P)$  and  $\chi_{c1}(1P)$* , PoS (Confinement X) 339, 2012; arXiv:1205.5703.
- [47] E. V. Veliev, H. Sundu, K. Azizi, and M. Bayar, *Scalar quarkonia at finite temperature*, Phys. Rev. D **82**, 056012 (2010).
- [48] H. X. Chen, Y. X. Yan, and W. Chen, *Decay behaviors of the fully bottom and charm tetraquarks*, Phys. Rev. D

- 106**, 094019 (2022).
- [49] Q. Xin and Z. G. Wang, *Analysis of doubly charmed tetraquark molecular states with the QCD sum rules*, Eur. Phys. J. A **58**, 118 (2022).
- [50] Q. N. Wang, W. Chen, and H. X. Chen, *Exotic molecular states and tetraquark states with  $J^P = 0^+$* , Chin. Phys. C **45**, 093102 (2021).